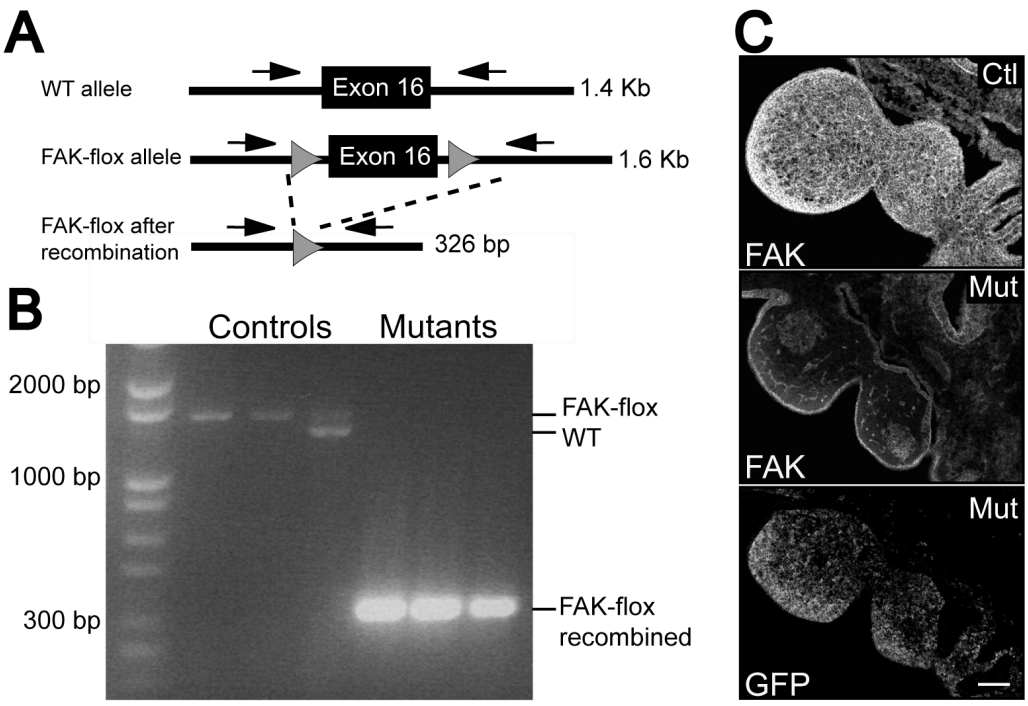

Supplemental Figure 1. Specific ablation of FAK in neural crest cells.
A. Schematic diagrams of the *fak* wild type gene (WT), the mutant *fak* allele with loxP sites inserted surrounding exon 16 (FAK-flox), and the mutant *fak* allele following Cre-mediated deletion of exon 16 are illustrated. Gray arrowheads depict locations of loxP sites surrounding exon 16, the second of two exons that encode the tyrosine kinase domain. Arrows represent primers used for allele identification using PCR genotyping. Expected sizes of PCR products are shown on the right. **B.** PCR analysis of lower mandible DNA from P0 *Wnt1cre*; $fak^{flox/flox}$ mutants and control littermates. In controls ($fak^{flox/flox}$, $fak^{flox/flox}$. $fak^{+/flox}$), bands representing wild-type (1.4 kb) and floxed (1.6 kb) alleles were observed. In *Wnt1cre;* $fak^{flox/flox}$ mutants only the Cre-recombined allele (326 bp) was detected. **C.** Evaluation of *Wnt1cre*-mediated recombination of the conditional *fak* allele. Immunohistochemistry of FAK shows expression in the mesenchyme and ectoderm of the 1st and 2nd branchial arches in control E10.5 embryos, whereas in *Wnt1cre;* $fak^{flox/flox}$ embryos mesenchymal expression is abolished but ectodermal expression persists. NCC detection by GFP in a *Wnt1cre;* $fak^{flox/flox}$*; Z/EG* embryo (bottom) shows that branchial arch mesenchyme is primarily NCC-derived, whereas there is no NCC contribution to ectoderm. Ctl, control; Mut, *Wnt1cre;* $fak^{flox/flox}$ mutant. Scale bar: 50 μm.

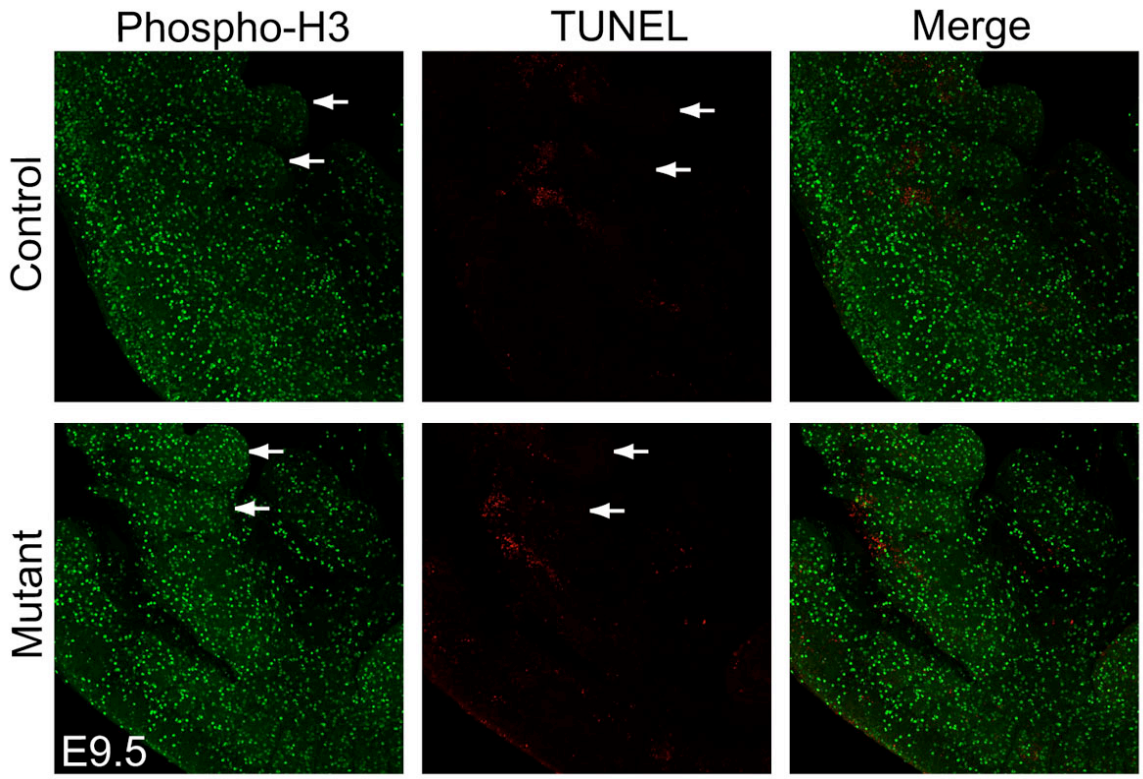

Supplemental Figure 2. Proliferation and death in E9.5 embryos.
E9.5 confocal stacks from control (**A**) and conditional *fak* mutant (**B**) embryos, showing overall similar proliferation (phospho-histone H3) and cell death (In Situ Cell Death Detection Kit) in the branchial arches 1 and 2 (arrows). Serial confocal sections were taken in embryos cleared with methylsalicilate.

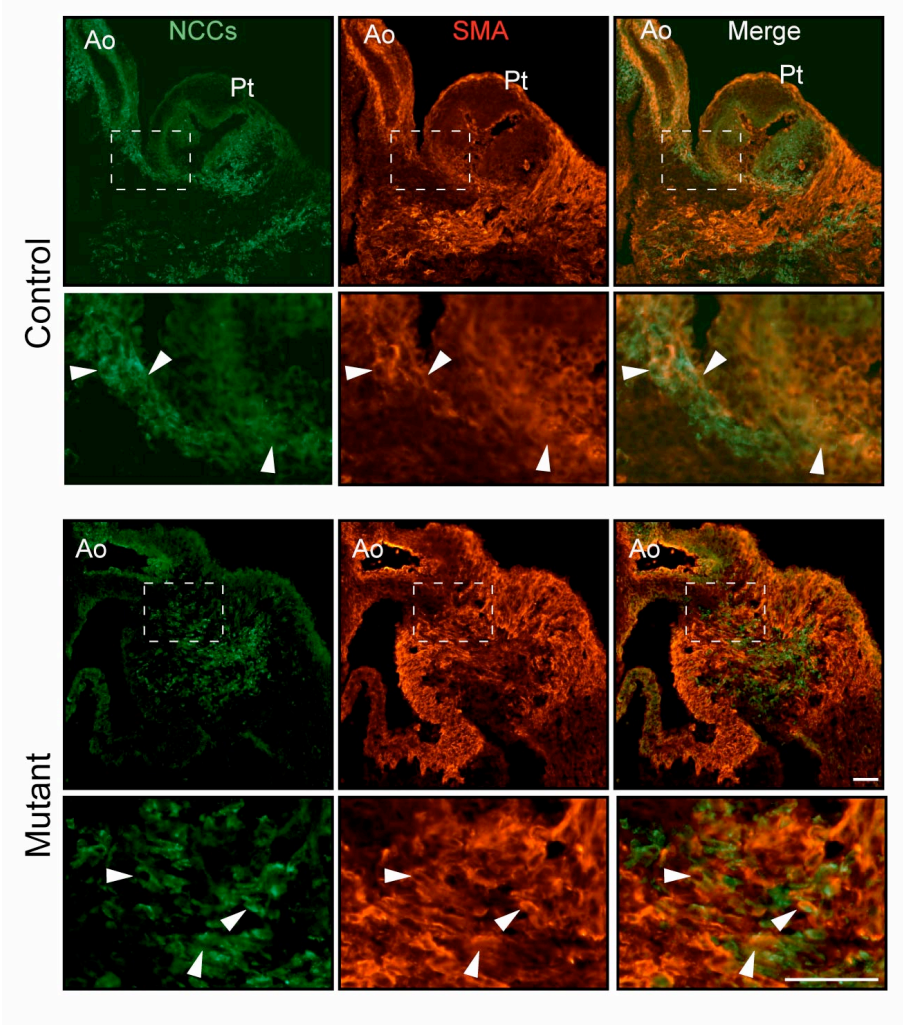

Supplemental Figure 3. Differentiation of NCCs in E12.5 outflow tracts.

E12.5 sagittal sections from control and conditional *fak* mutant embryos, showing normal differentiation of NCCs into smooth muscle in the proximal outflow tract region of mutant embryos, even when an abnormal aorticopulmonary comunication is present. Green shows expression of β-galactosidase by NCCs. Lower panels show higher magnification images from boxed areas. Note that in control and mutant embryos only a subset of NCCs in this region express SMA. Ao, aorta; Pt, pulmonary trunk. Scale bars: 50 μm

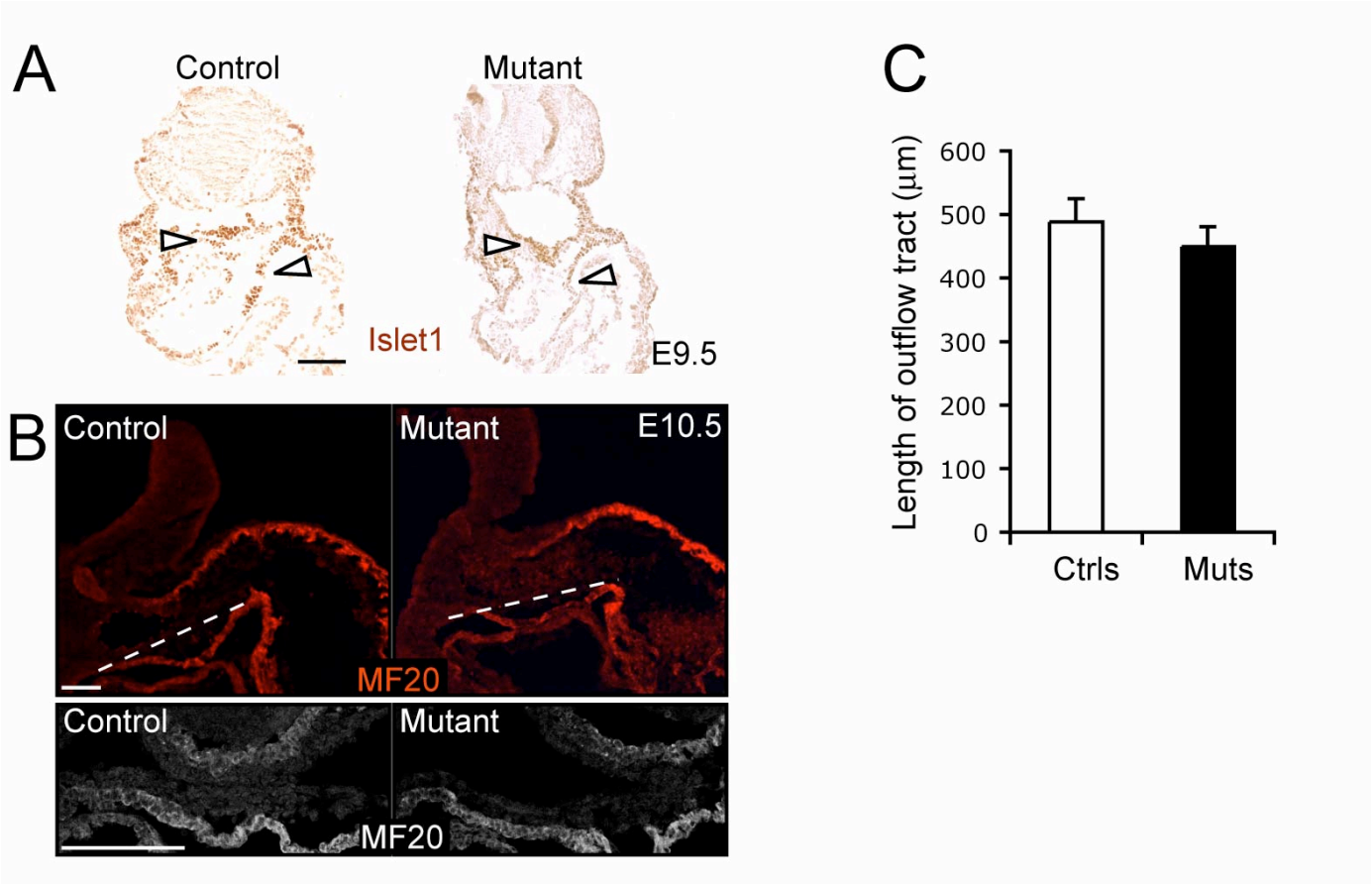

Supplemental Figure 4. Normal migration of secondary heart field cells in *Wnt1cre; fak*$^{flox/flox}$ **embryos.**

A. E9.5 cross sections from control and conditional *fak* mutant embryos, showing normal migration of secondary heart field cells to the outflow tract region (arrowheads). Secondary heart field cells were detected by immunostaining for Islet1 protein. **B.** E10.5 sagittal sections from two control and two *fak* mutants stained for MF20 to show the conotruncal myocardium in the outflow tract region derived from secondary heart field cells. Lower panels in B depict higher magnification images of MF20 immunostaining in the same regions from a different set of control and mutant embryos. **C.** Outflow tract length was measured in E10.5 embryos (dashed lines in upper panels in B). No significant differences were found between *fak* mutant embryos and control littermates (n=4). Scale bars: 100 μm

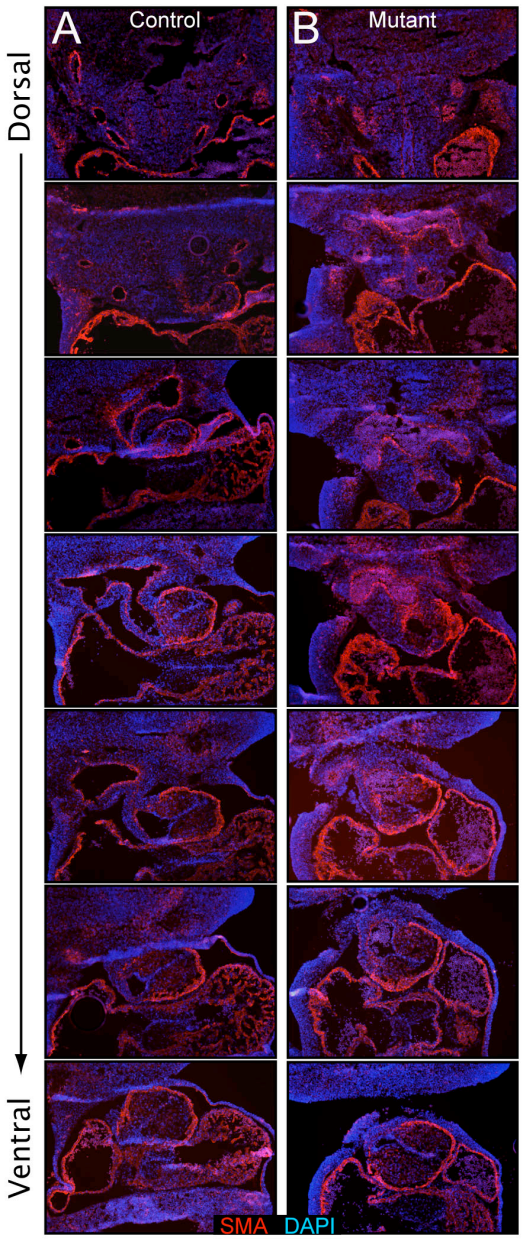

Supplemental Figure 5. E11 frontal sections used for Clay model illustrations.

Representative control (A) and mutant (B) cryostat sections showing branchial arch arteries and distal outflow tract. Red shows smooth muscle actin staining (SMA) and blue shows nuclei (DAPI). Plane of section is the same as in Figure 3G.

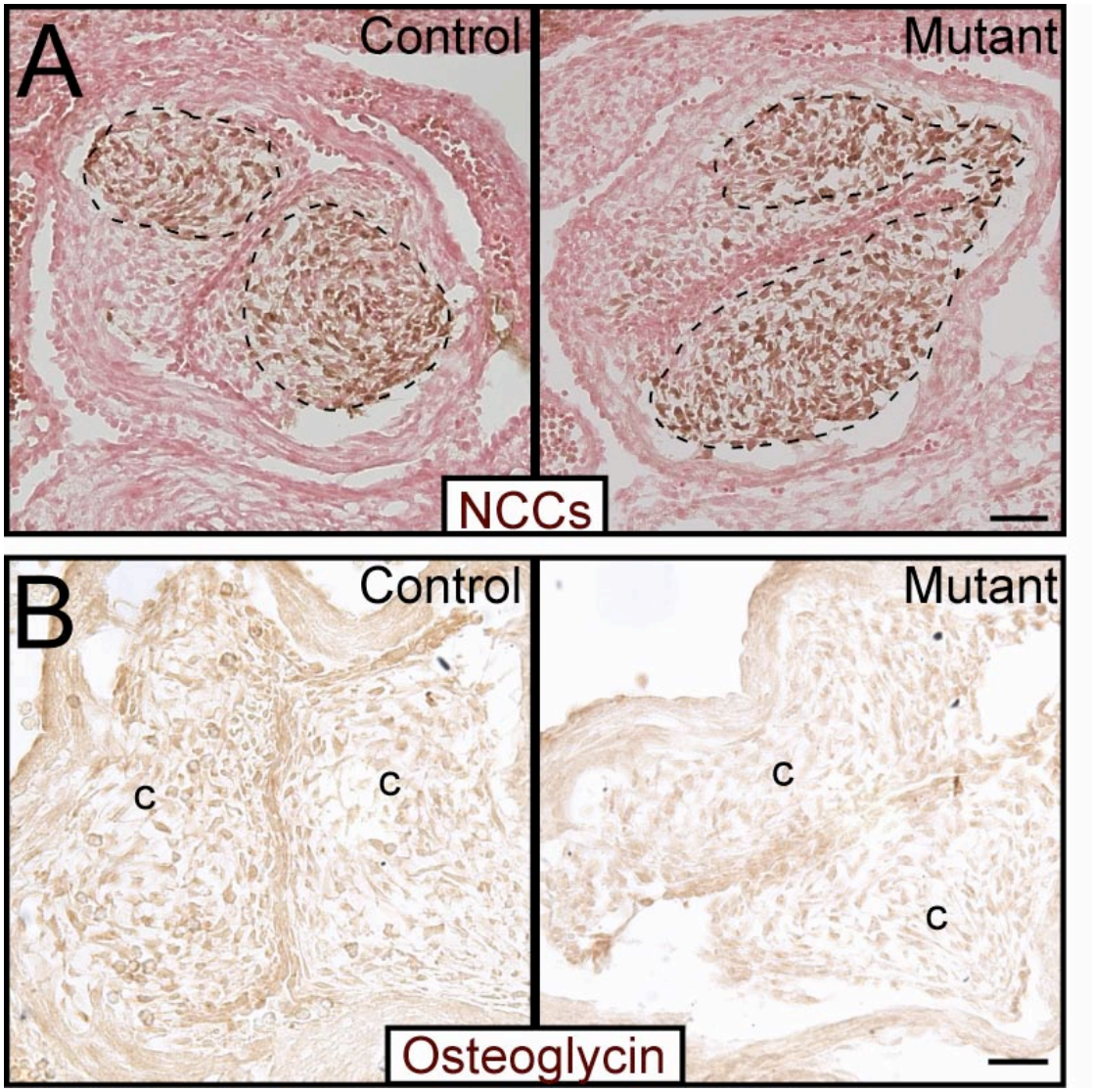

Supplemental Figure 6.

A) E11 frontal sections of *Wnt1cre; fak*$^{+/flox}$*; Z/EG* (Control) and *Wnt1cre; fak*$^{flox/flox}$*; Z/EG* (Mutant) embryos immunostained for GFP and counter stained with nuclear fast red to show NCC organization in the conotruncal cushions. Compared to controls, mutant NCCs are more scattered throughout the cushions and show less consistent polarity. This data further support our interpretation of abnormal NCC organization in fak mutant embryos. Dashed lines show NCC limits in the conotruncal cushions. **B)** Osteoglycin immunohistochemistry in the conotruncal cushions of E11 outflow tracts. E11 frontal sections from control and conditional *fak* mutant embryos, showing reduced expression of osteoglycin in *fak*-deficient NCC in the conotruncal cushions (c). Scale bars: 50 μm

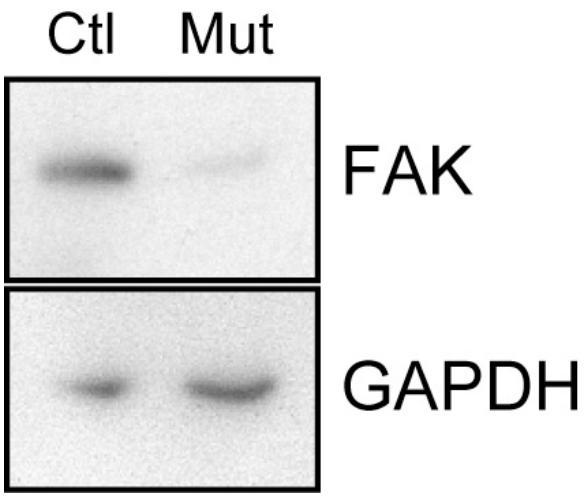

Supplemental Figure 7. Western blot analysis from Control (Ctl) and mutant (Mut) NCC cultures showing efficient downregulation of FAK in NCCs from conditional *fak* mutant embryos.

Supplemental Table 1. Genotype distribution of offspring from FAK+/flox;Wnt1Cre x FAKflox/flox crosses

Genotype	E8.5-E9.5 (n=105)	E10.5-E14.5 (n=201)	E16.5-E20 (n=85)	Embryonic (n=391)	P0-P2 (n=72)	P30 (n=54)
FAKflox/flox;Wnt1Cre	24 (23%)	54 (27%)	20 (24%)	98 (25%)	9 (13%)	1 (2%)
FAK+/flox;Wnt1Cre	28 (27%)	40 (20%)	24 (28%)	92 (24%)	28 (39%)	19 (35%)
FAKflox/flox	30 (29%)	51 (25%)	17 (20%)	98 (25%)	13 (18%)	21 (39%)
FAK+/flox	23 (22%)	56 (28%)	24 (28%)	103 (26%)	22 (31%)	13 (24%)

Supplemental Table 2. RNA profile analysis of E11 outflow tract transcripts.

Gene	Symbol	ID	Microarray	qPCR	Description
Osteoglycin	Ogn	NM_008760	-2.64	-3.78	Modulates collagen fibrillogenesis. Component of the vascular matrix.
Stathmin-like 3	Stmn3	NM_009133	-1.87	-2.11	Microtubule destabilizing factor. Negative regulator of Rac protein signal transduction
Paired related homeobox 1	Prrx1	NM_001025570	-1.74	-1.96	Prrx1 expression is induced by FAK. Expressed in endocardial cushions from E8.5. Knockout mice have vascular abnormalities.
PTK2 protein tyrosin kinase 2	FAK	NM_007982	-1.52	-1.75	Cytoplasmic tyrosine kinase activated by integrins and growth factors. Involved in cell motility, proliferation, apoptosis and ECM organization.
L1 cell adhesion molecule	L1cam	NM_008478	-1.62	-1.75	Cell adhesion molecule involved in neuron-neuron adhesion and neurite outgrowth. Binds b1-integrins and neuropilin.
Doublecortin	DCX	NM_178151	-1.41	-1.72	Asociates with actin filaments and microtubules. Regulates organization and stability of microtubules.
Perlecan	Hspg2	NM_008305	-1.62	-1.39	Coreceptor of FGF2. TGFb signaling upregulates Hspg2 transcription. Knockout mice have abnormal outflow tract rotation with abundant NCCs
Phosphatidylinositol -4-Phosphate	Pip5k1b	NM_008847	-2.14	-1.32	Mediates RAC1-dependent reorganization of actin filaments. Contributes to the activation of PLD2. Interacts with ARF1, RAC1, PLD1 and PLD2
Semaphorin 3C	Sema3c	NM_013657	+2.14	+1.37	Ablation of Sema3C results in cardiovascular malformations. Promotes neural crest cell migration into the proximal outflow tract.

Supplemental Table 3. Primers used for qPCR

Gene	Forward	Reverse
Stmn3	CCAGCACCGTATCTGCCTACA	GCTGAGAGTAGAAGCAGGAGCAA
Prrx1	GCCAGAGTGCAGGTGTGGTT	ACAGCAGTCACGTCTCCTGAGTAG
L1cam	TGCTCATACAGATTCCAGACGAATATA	CATTTCAGGCTTATGTCATCTGTTG
DCX	CAGCATCTCCACCCAACCA	TCATCCGTGACCCTCTCATATTT
Hspg2	AGAGGTGTGCCCCAGGTTACT	CTGGCACCTGACCATCTCTGT
Pip5k1b	CATCCAGTTAGGCATCACTCACA	TGTCAGGTTGCTGCCTTCACT
Sema3c	CATGATTGCAAGAATATGCCCTAAT	ACTGAGCATACAAGTCTTGCCTTTAA
GAPDH	GAGATCAACACGTACCAGTGCAA	TACACTCCACCACGTAGGGATTC
B2M	CTGCAGAGTTAAGCATGCCAGTA	TGATCACATGTCTCGATCCCAGTA